Biomechanical analysis of neochordal repair error from diastolic phase inversion of static left ventricular pressurization

Matthew H. Park, MS,[a,b] Mateo Marin-Cuartas, MD,[a,c] Annabel M. Imbrie-Moore, PhD,[a,b] Robert J. Wilkerson, BS,[a] Pearly K. Pandya, BS,[a,b] Yuanjia Zhu, MD, MS,[a,d] Hanjay Wang, MD,[a] Michael A. Borger, MD, PhD,[c] and Y. Joseph Woo, MD[a,d]

ABSTRACT

Objective: Neochordal implantation is a common form of surgical mitral valve (MV) repair. However, neochord length is assessed using static left ventricular pressurization, leading surgeons to evaluate leaflet coaptation and valve competency when the left ventricle is dilating instead of contracting physiologically, referred to as diastolic phase inversion (DPI). We hypothesize that the difference in papillary muscle (PM) positioning between DPI and physiologic systole results in miscalculated neochord lengths, which might affect repair performance.

Methods: Porcine MVs (n = 6) were mounted in an ex vivo heart simulator and PMs were affixed to robots that accurately simulate PM motion. Baseline hemodynamic and chordal strain data were collected, after which P2 chordae were severed to simulate posterior leaflet prolapse from chordal rupture and subsequent mitral regurgitation. Neochord implantation was performed in the physiologic and DPI static configurations.

Results: Although both repairs successfully reduced mitral regurgitation, the DPI repair resulted in longer neochordae (2.19 ± 0.4 mm; $P < .01$). Furthermore, the hemodynamic performance was reduced for the DPI repair resulting in higher leakage volume ($P = .01$) and regurgitant fraction ($P < .01$). Peak chordal forces were reduced in the physiologic repair (0.57 ± 0.11 N) versus the DPI repair (0.68 ± 0.12 N; $P < .01$).

Conclusions: By leveraging advanced ex vivo technologies, we were able to quantify the effects of static pressurization on neochordal length determination. Our findings suggest that this post-repair assessment might slightly overestimate the neochordal length and that additional marginal shortening of neochordae might positively affect MV repair performance and durability by reducing load on surrounding native chordae. (JTCVS Techniques 2022;12:54-64)

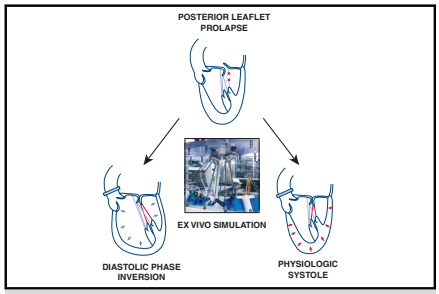

Robotic ex vivo simulation of static pressurization assessment for neochordal repair.

CENTRAL MESSAGE

Neochord length might be overestimated during static pressurization testing of post-repair mitral valve competency because of diastolic phase inversion of ventricular geometry, altering biomechanics.

PERSPECTIVE

We quantified neochord length error from diastolic phase inversion of left ventricular geometry due to static pressurization, with the finding that this assessment of post-repair competency might overestimate neochord length leading to reduced hemodynamic and chordal repair performance. Surgeons should be aware of this error when adjusting neochordae, and marginal shortening might improve repair performance.

From the Departments of [a]Cardiothoracic Surgery, and [b]Mechanical Engineering, Stanford University, Stanford, Calif; [c]University Department of Cardiac Surgery, Leipzig Heart Center, Leipzig, Germany; and [d]Department of Bioengineering, Stanford University, Stanford, Calif.

This work was supported by the National Institutes of Health, United States (R01 HL089315-01 and R01 HL152155; Y.J.W.), the National Science Foundation Graduate Research Fellowship Program, United States (DGE-1656518; A.M.I.-M.), the Stanford Graduate Fellowship (A.M.I.-M.), and the Thoracic Surgery Foundation Resident Research Fellowship, United States (Y.Z.), and a generous donation from Kevin Taweel to support this research effort.

Matthew H. Park and Mateo Marin-Cuartas contributed equally to this work.

Received for publication July 27, 2021; accepted for publication Jan 12, 2022; available ahead of print Jan 26, 2022.

Address for reprints: Y. Joseph Woo, MD, Department of Cardiothoracic Surgery, Department of Bioengineering, Stanford University, Falk Cardiovascular Research Building CV-235, 300 Pasteur Drive, Stanford, CA 94305-5407 (E-mail: joswoo@stanford.edu).

2666-2507

https://doi.org/10.1016/j.xjtc.2022.01.009

Abbreviations and Acronyms

CT = computed tomography
DPI = diastolic phase inversion
e-PTFE = expanded polytetrafluoroethylene
FBG = Fiber Bragg Grating
IPM = image-guided papillary muscle
LV = left ventricle
MR = mitral regurgitation
MV = mitral valve
PM = papillary muscle

▶ Video clip is available online.

Mitral valve (MV) prolapse is a common disease characterized by a combination of elongated or ruptured chordae tendineae, excessive leaflet tissue, and annular dilation. These pathologic changes often result in mitral regurgitation (MR) requiring surgery, and US prevalence estimates of this disease range from 2% to 15% and up to 35% in some studies.[1] The standard of care is increasingly prioritizing surgical repair over replacement, because repair is considered superior in terms of patient survival, left ventricular function, and freedom from reoperation for many patients.[2-8] Surgical repair in this context commonly involves chordal replacement via artificial neochord implantation using expanded polytetrafluoroethylene (e-PTFE) sutures, spanning from the leaflet to the papillary muscle (PM), which has shown excellent clinical results.[9,10]

The most common difficulty with neochordal repair is determining the optimal length of the artificial neochordae.[11] To help mitigate this challenge, surgeons often deliver saline to the left ventricle (LV) using a suction irrigation device or syringe to visually inspect leaflet coaptation and valve competency and to appropriately adjust the neochord length (Video 1). Although this static LV pressurization assessment technique, also known as the saline or waterproof test, can help surgeons to approximately estimate neochord length, there exists a critical source of error involved in this method. When pressurizing the LV of an arrested heart, the MV apparatus and subvalvular structures dilate in a state similar to that of diastole when the LV would otherwise be contracting during systole in a beating heart.[12,13] More specifically, in vivo, the PMs, which commonly serve as the distal anchor point of the neochordae, move with each heartbeat, translating and rotating relative to the valve annulus, and this movement can be generally characterized as a reduction in the distance between the PM and the valve annulus upon leaflet coaptation.[14,15] On the contrary, static pressurization simulates the opposite as it causes the LV to dilate, moving the PMs further away from the annulus upon leaflet coaptation. This phenomenon, which we refer to as the diastolic phase inversion (DPI), means that neochord length assessment occurs when the PMs are further away from the valve leaflets than what would otherwise be the case upon coaptation during systole (Figure 1). We hypothesize that the difference in PM positioning during DPI from static pressurization compared with that during physiologic systole results in longer implanted neochord lengths, which in turn might affect hemodynamic performance and chordal stresses of the repair. By simulating these conditions in an ex vivo left heart simulator using our advanced image-guided PM (IPM) robotic system, we aimed to quantify this error and evaluate the hemodynamic and biomechanical performance of MV repair in the presence of DPI (Figure 2). Through these experiments, we hope to further elucidate the intricacies of artificial neochord implantation and to provide mechanical guidance on repair performance.

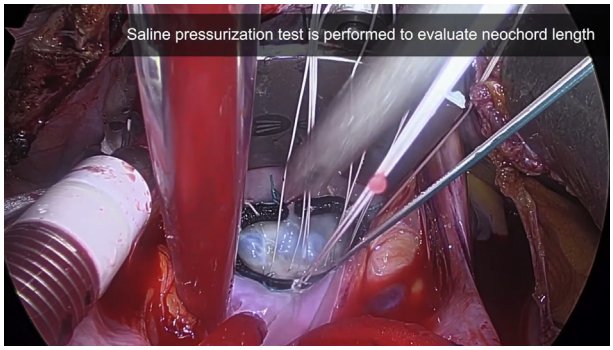

VIDEO 1. Intraoperative video highlighting the use of static left ventricular pressurization, or the saline test, during neochordal mitral valve repair. Video available at: https://www.jtcvs.org/article/S2666-2507(22)00037-2/fulltext.

METHODS

IPM Robotic System

Using our previously validated IPM robotic system, we can mimic the precise motion of PMs throughout the cardiac cycle (Figure 3, *A*).[15] The robotic actuators were designed as a modified Stewart platform system consisting of 6 servo motors and actuating rods connecting to an end-effector platform. This design allowed us to create a high-bandwidth system with 6 degrees of freedom (3 rotational and 3 translational) to fully capture the native kinematics of the PMs, and advanced mathematical analyses and supercomputing simulations were used to precisely tune design parameters. Three-dimensional validation tests revealed a low spatial error in recreating 6 degrees of freedom motion. These robots were incorporated in our ex vivo left heart simulator, and the PM of explanted porcine MVs were mounted to the IPM end-effectors as precise cycle timing was synchronized with the linear piston pump. The motion of this robotic system was prescribed by high-resolution human computed tomography (CT) imaging, which generates a more physiologically accurate simulation. The CT imaging data were acquired from a deidentified data set of high-resolution scans of an adult human heart with 10 images over the course of 1 cardiac cycle. To determine the physiologic motion of the PMs, the MV annulus and PMs

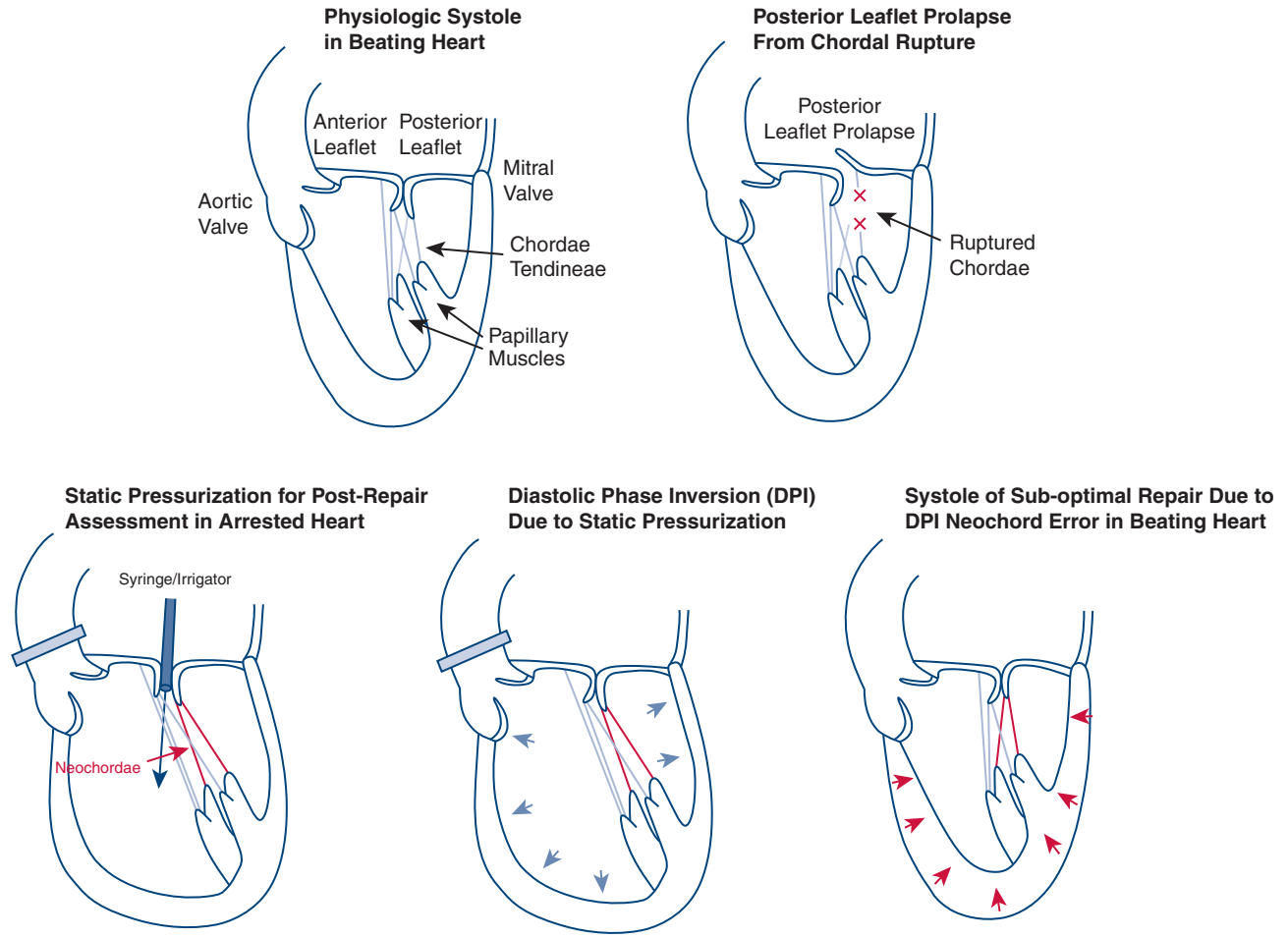

FIGURE 1. Labeled illustration of mitral valve neochordal repair with static pressurization for post-repair assessment and diastolic phase inversion (*DPI*). We hypothesize that DPI results in neochord length overestimation, which might lead to a suboptimal repair and reduced hemodynamic performance.

were tracked using CEMRG software (Cardiac Electro-Mechanics Research Group), and the PM trajectories were adjusted to compensate for the native motion of the annulus, setting the inertial reference frame to that of the annulus, as the annulus is fixed in our ex vivo simulator.[15] Our IPM robotic system represents a significant advancement for ex vivo simulation, enabling more reliable cardiac simulations and repair optimizations. More importantly, the development of such a system empowers our research group to quantify a new regime of cardiac biomechanics because PM positioning and motion are crucial components to simulating and exploring novel experimental questions such as that of DPI.

Left Heart Simulator Testing

MVs (n = 6) were carefully explanted from porcine hearts obtained fresh from an abattoir (Animal Technologies) in accordance with institutional guidelines and mounted in a left heart simulator using a 3D-printed silicone sewing ring (SIL 30), and the PMs were affixed to the IPM robots, as previously described (Figure 3, *B*).[15,16] The left heart simulator flow loop features a pulsatile linear piston pump (ViVitro Superpump; ViVitro Labs) used to generate physiologic hemodynamics for the valve; the pump controller and software (ViVitest Software; ViVitro Labs) are programmed in accordance with ISO 5840 standards for in vitro valve testing.[17] The heart simulator features an electromagnetic flow probe (Carolina Medical Electronics) positioned to record MV flow; 0.9% normal saline was used as the test fluid to ensure proper transduction of the flow probe. Ventricular, aortic, and atrial pressures were measured using pressure transducers (Utah Medical Products Inc). The linear piston pump was programmed to generate an effective stroke volume of 70 mL at 70 beats per minute. The heart simulator also features 2 compliance chambers as well as adjustable peripheral resistance; both were titrated at baseline to produce a mean arterial pressure of 100 mm Hg (systolic 120 mm Hg, diastolic 80 mm Hg). For each test, hemodynamic data were collected and averaged across 10 cardiac cycles.

Additionally, high-resolution Fiber Bragg Grating (FBG) sensors (DTG-LBL-1550 125 μm FBGS International) were implanted in P1 and P3 primary and secondary chordae to directly measure forces on the surrounding chordae (Figure 3, *C*). These sensors have been used and validated for measuring chordal stress in ex vivo and in vivo settings, elucidating numerous novel insights.[16,18-20] The FBG optical strain sensors were calibrated to correlate strain to force using an Instron 5848 Microtester with a 20-N load cell as previously described.[16] FBG measurements were recorded at a sampling frequency of 1000 Hz with an optical interrogator (Micron Optics si255 with ENLIGHT, Micron Optics), and force data of the chordae were analyzed using a variety of data analysis and signal processing libraries using Python (Python Software Foundation).

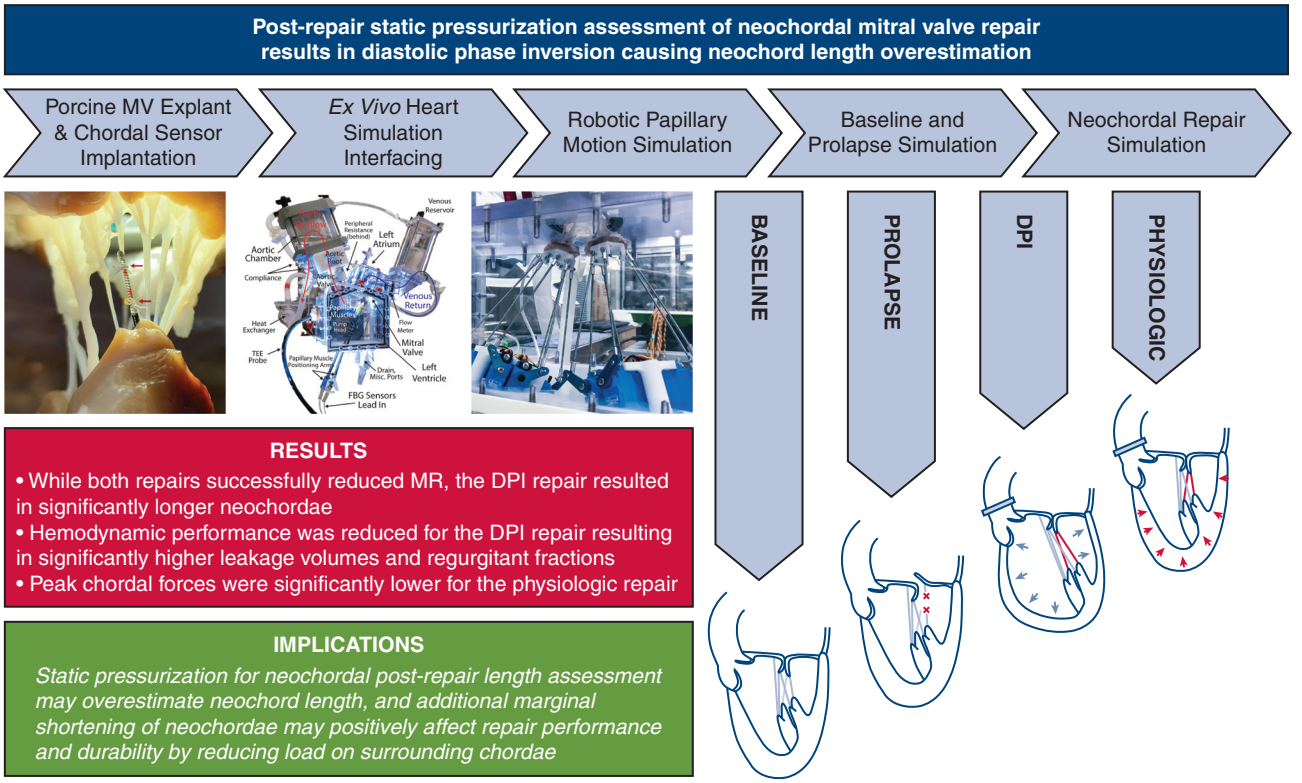

FIGURE 2. The study's methods, results, and implications. Experimental design to test the effects of diastolic phase inversion (*DPI*) of left ventricular geometry after static pressurization for assessment of post-repair mitral valve (*MV*) competency. Explanted porcine MVs were mounted in our robotic ex vivo simulator with implanted chordal strain gauges (n = 6). Four paired experiments were tested on each valve in the simulator: baseline control, prolapse, DPI repair, and physiologic repair. *TEE*, Transesophageal echocardiography; *FBG*, Fiber Bragg Grating; *MR*, mitral regurgitation.

To conduct our experiment, hemodynamic and chordal strain data were collected for all control and experimental conditions, whereas PM motion was initially calibrated for the control condition and remained unchanged throughout each experiment. PM motion was used in conjunction with pulsatile physiologic simulation whenever valve testing and data recording occurred. First, healthy explanted porcine MVs were mounted and run in our simulator, which we refer to as the baseline condition and which serves as the control. Next, P2 chordae were severed to simulate posterior leaflet prolapse from chordal rupture and subsequent MR, which is referred to as the prolapse condition. After the induction of prolapse, the valve was

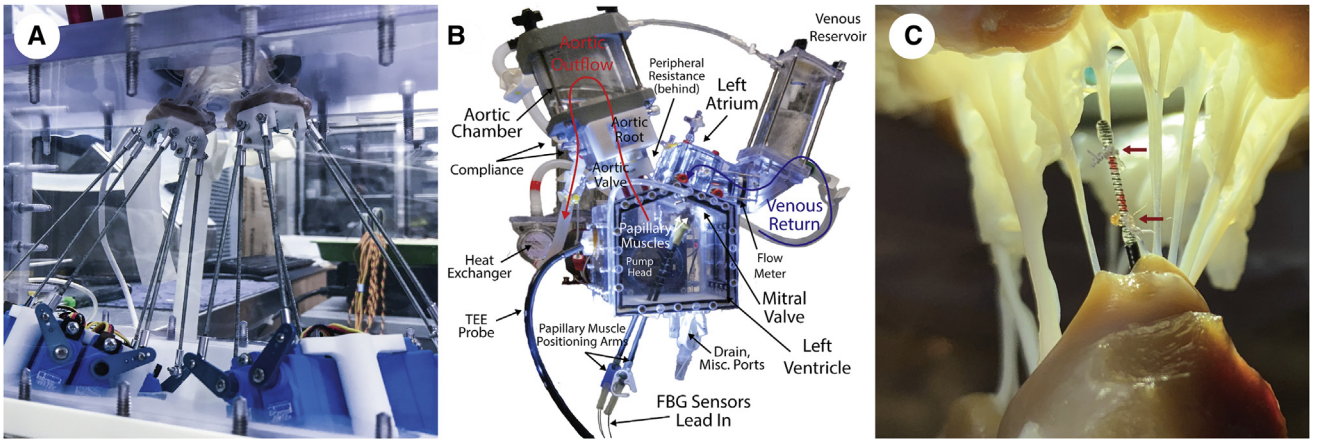

FIGURE 3. Heart simulator experimental setup, from Imbrie-Moore. A, Picture of the image-guided papillary muscle robotic system sewn to papillary muscles of a porcine mitral valve to mimic the motion of the heart. B, Diagram of the custom left heart simulator with stationary papillary muscles during ex vivo cardiac simulation experiments. C, High-resolution Fiber Bragg Grating strain gauge sensor instrumenting a chordae tendineae; the sensor is calibrated to correlate strain to force. The chord is severed between the 2 suture attachment points, denoted by *red arrows*, to transmit all force through the sensor. Reproduced with permission from the Royal Society.[15]

statically repaired in 2 configurations in a randomized order. The first, which we refer to as the physiologic repair, represents the repair in which the PMs were positioned in the physiologically accurate locations that corresponded to the time domain of leaflet coaptation during peak systole, confirmed by healthy, human CT imaging. The second, which we refer to as the DPI repair, represents the repair commonly implemented in a real operating room setting in which static LV pressurization is used to assess leaflet coaptation, inducing DPI and the associated geometric error. This state corresponds to a PM positioning locus similar to that found in end diastole, as the dilation of the heart upon LV pressurization can be correlated to the diastolic geometry of the heart. The static PM position was again confirmed using the CT images and translated to the ex vivo simulator via IPM robotic control, where artificial neochordal implantation was performed. Neochord implantation using e-PTFE, CV-5 suture, and the standard interrupted neochord technique was performed in the physiologic and DPI stationary PM configurations and through the same PM and leaflet anchoring loci, after which the valves were reanalyzed in the simulator using the originally calibrated PM trajectories.

Statistical Analysis

Continuous variables are reported as mean ± standard error. To account for non-normally distributed forces as well as the multistaged experimental design, nonparametric Friedman tests with pairwise comparisons were used to compare continuous variables between groups. For pairwise comparisons of cardiac output between the DPI and physiologic repairs, we assumed a normal distribution based on Shapiro-Wilk acceptance of the null hypothesis and used a paired Student *t* test for comparison.

RESULTS

Hemodynamic data confirmed that cutting P2 chordae successfully induced MR. The mean arterial pressure (74.7 ± 2.8 mm Hg vs 99.4 ± 1.1 mm Hg; $P < .01$) and cardiac output (4.2 ± 0.23 L/min vs 5.4 ± 0.3 L/min; $P = .01$) were lower for prolapse compared with baseline. Moreover, the mitral leakage volume (18.4 ± 4.5 mL vs 1.1 ± 0.5 mL; $P < .01$) and regurgitant fraction (31.2 ± 3.8% vs 9.0 ± 0.9%; $P < .01$) were higher for prolapse compared with baseline. Mean flow and pressure tracings over a cardiac cycle for the 4 stages of the experiment (baseline, prolapse, DPI repair, and physiologic repair) are shown in Figure 4, *A* and *B*, respectively, with the shaded regions representing standard error.

For our experimental conditions, the physiologic and DPI repairs were successful in eliminating regurgitation. Mitral leakage volume was reduced from the prolapse value of 18.4 ± 4.5 mL to 2.1 ± 0.1 mL ($P < .01$) for the physiologic repair and 3.6 ± 0.5 mL ($P < .01$) for the DPI repair. Moreover, pressures were restored for both repairs with similar mean arterial pressures ($P > .8$) and cardiac output ($P > .7$) between the repairs and baseline levels. However, we also found that the DPI repair resulted in significantly longer neochordae compared with those of the physiologic repair (2.2 ± 0.4 mm longer, an increase of 16.0%; $P < .01$). This difference in neochord length had downstream effects on the hemodynamics as well. Although both repairs adequately reduced MR, the physiologic repair resulted in marginally reduced MR (2.3 ± 0.6%; $P < .01$, reported as difference) and leakage volume (1.5 ± 0.4 mL; $P = .01$,

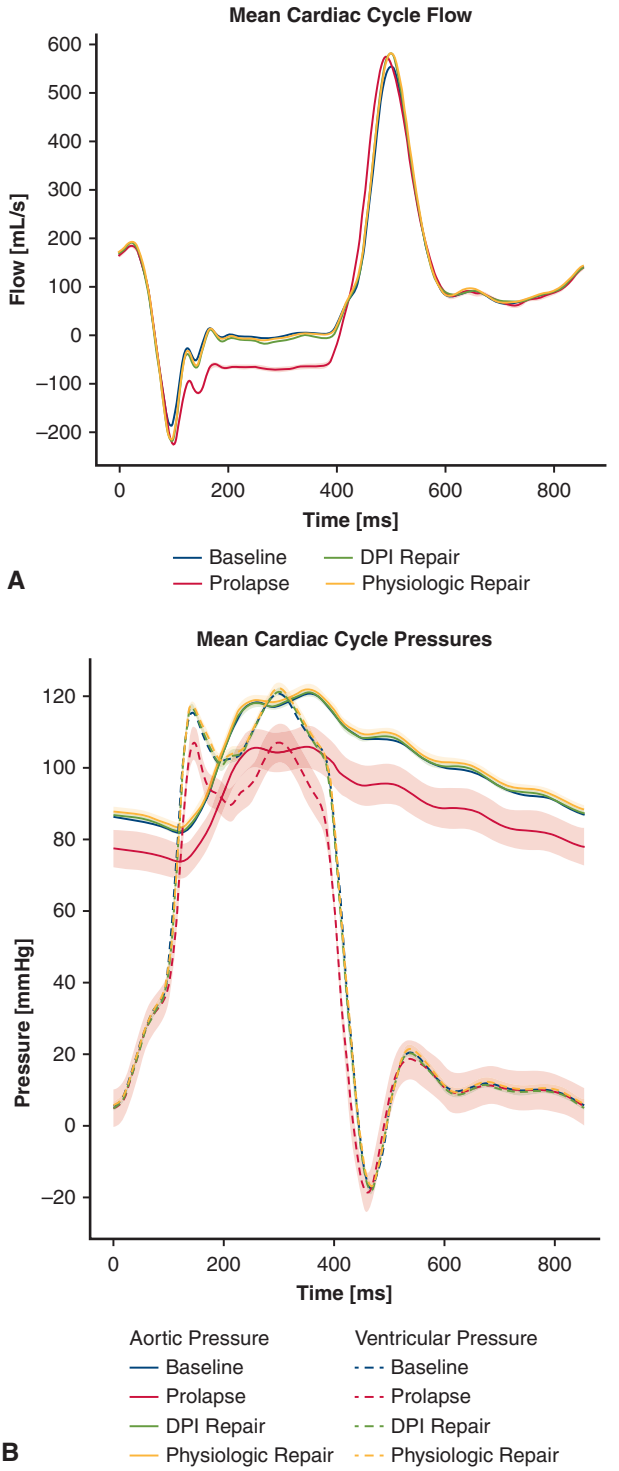

FIGURE 4. A, Mean flow tracings for baseline, prolapse, diastolic phase inversion (*DPI*) repair, and physiologic repair. Flow tracings show successful induction of mitral regurgitation for the prolapse condition followed by restoration of flow dynamics for both repairs. B, Mean pressure tracings for all experimental conditions. Pressure data shows a reduction in pressures for the prolapse condition, indicating successful induction of mitral regurgitation, followed by a return to normal pressures for both repair conditions. *Shaded regions* for both panels represent standard error.

reported as difference) and marginally increased cardiac output (0.2 ± 0.1 L/min; $P < .05$, reported as difference) compared with those of the DPI repair.

Figure 5, *A* shows native P1 and P3 mean primary and secondary chordal forces over the time domain of a single cardiac cycle for both repair conditions, where the shaded regions represent standard error. In the aggregate, peak native chordal forces were reduced ($P < .01$) in the physiologic repair (0.57 ± 0.11 N) compared with those in the DPI repair (0.68 ± 0.12 N). These chordal force results correspond to a 0.11 ± 0.04 N or 16.4% reduction in forces on average for the physiologic repair compared with those of the DPI repair. Figure 5, *B* shows the box plot of peak chordal forces with median and interquartile range for both repair conditions. Full hemodynamic, chordal force, and neochordal length data for all experimental conditions can be found in Table E1.

DISCUSSION

Leveraging advances in ex vivo heart simulation technology, we used precision robotics to biomechanically quantify the error involved in DPI from static LV pressurization assessment during artificial neochordal implantation. Our results provide novel insights for better understanding this surgical procedure, with deeper implications on optimizing repair performance. By bringing a strong mechanical foundation to techniques developed by surgeon experimentation and preferences in the operating room, we have expanded on the technical corpus of heart surgery aiming to translate our ex vivo work to meaningful improvements and optimizations in the clinic and for patient health and safety.

Although both repairs successfully reduced MR, our results indicate that neochordal repair in the presence of the geometric error involved in DPI contributes to the higher leakage volume and regurgitant fraction levels seen in the DPI repair. Multiple hemodynamic metrics including regurgitant fraction, leakage volume, cardiac output, and energy loss all corroborate the reduction of hemodynamic performance of the simulated DPI repair. Furthermore, when we analyzed native chordal forces in the P1 and P3 regions of the MV, we observed an increase in peak forces in the DPI repair relative to those of the physiologic repair. Although we observed differences in our results, these differences were relatively small between conditions, which might suggest that the increased forces might not present a direct, acute danger to the repair. However, over long time durations, the additional forces might contribute to higher fatigue stresses and faster deterioration of the surrounding chordae, resulting in a less durable repair.[20-23] Small hemodynamic or mechanical changes in repair performance are significantly amplified in the context of extended time frames of long-term outcomes and durability, because of the repeated cyclic loading of cardiac systems and the cumulative properties of mechanical fatigue.

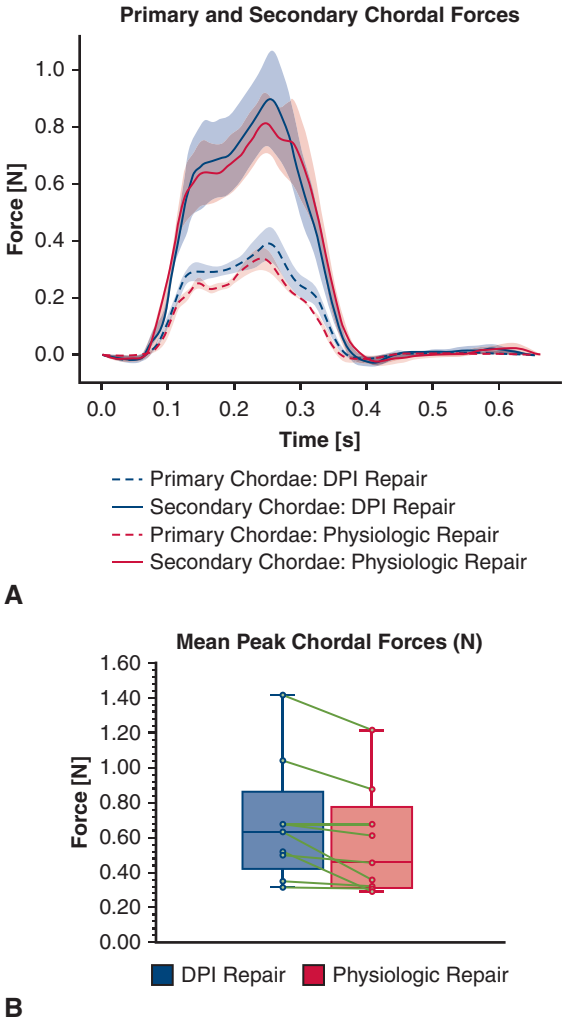

FIGURE 5. A, Mean force tracings for primary and secondary chordae in diastolic phase inversion (*DPI*) and physiologic repair conditions. A Fiber Bragg Grating sensor was used in each case to measure real-time native chordae forces. *Shaded regions* represent standard error. On average, the physiologic repair resulted in lower chordal forces than those of DPI repair, with peak force data additionally reflecting that reduction. B, Box plot of combined primary and secondary peak chordal forces for the DPI and physiologic repairs. The *upper and lower borders* of the box represent the upper and lower quartiles, the *middle horizontal line* represents the median, and the *upper and lower whiskers* represent the maximum and minimum values. *Lines between points* represent paired data. The peak forces were lower ($P < .01$) for the physiologic repair (0.57 ± 0.11 N) compared with the DPI repair (0.68 ± 0.12 N).

When applying this phenomenon to chordae, it has been shown that additional mechanical tension exponentially increases the rate of creep for these viscoelastic load-bearing structures.[24] This mechanism leads to a loss of organized collagen structure, inducing microcracks, which strongly suggests that spontaneous chordal rupture and elongation is caused by mechanical fatigue.

Additionally, although the DPI state during an intraoperative, flaccid ventricle saline injection is not truly analogous to physiologic diastole in the heart, which is an active myocardial process, we used the PM positioning of end diastole to dictate the DPI state in these experiments. However, the use of physiologic diastole to simulate the DPI state represents a lower bound of error because the LV is pressurized at much lower levels during end diastole compared with that of a static pressurization test. Studies that classified left ventricular end diastolic pressure via in vivo human left ventricular catheterization or echocardiography, indicate that left ventricular end diastolic pressure values range from 3 to 8 mm Hg for normal individuals, and 15 to 30 mm Hg or greater for patients with severe alveolar edema.[25,26] However, the pressures of static testing in the operating room during MV repair are meant to re-create the systolic configuration of the valve and often reach levels much greater than 30 mm Hg, indicating greater levels of PM distension and neochordal length error.

Although the explicit mechanistic causation is still speculative, our results indicate that the reduction of hemodynamic performance and the inferior chordal dynamics might be directly attributable to the relatively longer implanted neochord length of the DPI repair. Mechanically, a longer neochord corresponds to increased forces on the surrounding chordal architecture because e-PTFE as a suture material behaves in an elastic–plastic manner when loaded in uniaxial tension, prescribing an approximate Hookean elastic behavior of the neochord, and load distribution is complete and deterministic according to Newtonian mechanics.[27,28] Therefore, shorter neochordae result in improved performance because of increased neochordal loading and faster preload response. The increased loading reduces prolapse and leakage, whereas the faster response refers to how quickly the neochord loads relative to the time domain of the cardiac cycle. The marginally shorter neochord will load more and faster after the end of diastole, preventing regurgitation and improving the hemodynamic performance of the valve, all of which were corroborated by our results but will need to be validated by further in vivo studies.

Clinical Perspective

Our findings are the first, to our knowledge, to quantify neochordal length error when using static pressurization for post-repair assessment of MV competency. Although fidelity is lost in ex vivo experimentation, presenting challenges for extracting specific clinical guidance on the basis of our results, we can speculate that additional marginal shortening of the neochord might improve the chordal mechanics and hemodynamic performance of the repair, leading to a potentially more durable outcome. However, it is important to note that the amount of DPI error depends on the level of pressurization experienced by the LV during the saline test, with additional patient-specific variance due to left ventricular architecture, which means that the amount of additional shortening required for the repair will vary. We advise not overfilling the LV to avoid geometric changes that might induce further error upon evaluation. Additionally, although our experiments elucidate the difference between repairs in the presence of DPI and physiologic systole, further work is required to directly correlate and specifically quantify the amount of additional neochordal shortening in the presence of DPI to optimize repair performance, and as such care must be taken when generalizing our results, which do not directly indicate that any specific quantified amount of active shortening will lead to improved performance.

Limitation

Although we took many steps to accurately simulate and isolate the repair conditions experienced in the operating room, there were some crucial obstacles of note. Because heart surgery is very dependent on technique and preference, a primary concern of this work was surgeon variance. Although we tried to account for such variation by ensuring a single surgical operator for all repair experiments, it is difficult to extrapolate the specific length quantifications in these results to all operating conditions. Moreover, patient-specific left ventricular architecture and level of pressurization adds to the potential variability of neochord length during a repair. Although our surgical model remained robust and consistent throughout experimentation, neochordal length accuracy can be further optimized to account for pressure and geometric idiosyncrasies on a case-by-case basis. Specifically, we are currently exploring the use of patient-specific, image-based modeling to quantify DPI in real time, dependent on measured static left ventricular pressure loads. In doing so, we can provide immediate feedback to the surgeon estimating DPI error, enabling advanced, next-generation tooling for neochordal length determination.

Another limitation of our work was that porcine hearts were used with human CT data as a model for a human operating room scenario. However, we have taken care to isolate the MV apparatus and reduce the influence of porcine anatomical divergence by removing most of the surrounding left ventricular and atrial tissues. Moreover, we have taken considerable steps to provide a generalizable platform for accurate transfer of human CT data to our porcine model geometry. Primarily, we have engineered trajectory scaling on the basis of normalized anatomic geometric valve size, measured using standard valve sizing methods. This allows us to account for gross valve geometric differences for individual porcine valves.

It is additionally worth noting that chordal ruptures can be associated with severe, chronic MR with accompanying ventricular remodeling and alterations in subvalvular

geometry, and it is unclear whether physiologic and DPI PM positions retain the same relationship as that of normal human hearts. Although it is true that neochordal repair might occur in the context of chronic MR, the number of different chronic etiologies and the lack of comprehensive and generalizable degenerative ex vivo MR models makes testing this hypothesis difficult. Because this is, to our knowledge, the first documented experiment to study DPI induced during surgical repair, rather than simulating this condition across the entire spectrum of primary and degenerative MR etiologies, we instead chose to evaluate this condition using an isolated chordal rupture model, which describes the most common primary MR etiology. This allowed us to simplify our model, providing the foundational evidence for future expansions into a more holistic subset of degenerative models and surgical conditions, and the technical basis describing the DPI error.

Finally, another obstacle adding complexity to understanding repair performance is the effect of long-term, post-repair ventricular remodeling. This phenomenon might alter the long-term performance of the repair regardless of exact neochord length, and it is difficult to understand the effects without a longitudinal in vivo clinical evaluation. However, restoring hemodynamics and chordal loading to a state more similar to that of the baseline, healthy valve is estimated to have a positive effect on ventricular remodeling. This is because it has been shown that pathological mechanical changes and cues, such as increased wall stresses, can further aggravate the heart biology, causing complex signaling cascades that prompt the heart to further remodel.[29,30] Therefore, a more accurate reconstitution of the native, healthy biomechanics of the valve, guided by a greater understanding of DPI error, might additionally contribute to improved long-term outcomes of the repair.

CONCLUSIONS

DPI from static LV pressurization is a critical phenomenon to more closely investigate because it directly affects the mechanical performance of neochordal repair. By leveraging advanced, robotic ex vivo technologies and biomechanics analyses, we quantified the effects of static LV pressurization during the neochord length determination procedure. In the process of better understanding DPI, we have generated meaningful insights that might improve the clinical implementation of neochordal repair. Specifically, our findings suggest that DPI error might cause a slight overestimation of neochord length and that additional marginal shortening of neochordae might positively affect MV repair performance and durability by reducing load on surrounding native chordae and improving neochord mechanics. Future experimentation should incorporate patient-specific architecture and advanced modeling techniques to correlate left ventricular pressure load to real-time clinical tools that can be used to more precisely and accurately determine optimal neochord lengths, bringing an interdisciplinary, cutting-edge engineering approach to cardiothoracic surgery.

Conflict of Interest Statement

The authors reported no conflicts of interest.

The *Journal* policy requires editors and reviewers to disclose conflicts of interest and to decline handling or reviewing manuscripts for which they may have a conflict of interest. The editors and reviewers of this article have no conflicts of interest.

The authors thank Kevin Taweel for the generous donation to support this research effort.

References

1. Freed LA, Levy D, Levine RA, Larson MG, Evans JC, Fuller DL, et al. Prev alence and clinical outcome of mitral-valve prolapse. *N Engl J Med*. 1999;341: 1-7. https://doi.org/10.1056/NEJM199907013410101
2. Gillinov AM, Blackstone EH, Nowicki ER, Slisatkorn W, Al-Dossari G, Johnston DR, et al. Valve repair versus valve replacement for degenerative mitral valve disease. *J Thorac Cardiovasc Surg*. 2008;135:885-93, 893.e1. https://doi.org/10.1016/j.jtcvs.2007.11.039
3. Nishimura RA, Otto CM, Bonow RO, Carabello BA, Erwin JP, Guyton RA, et al. 2014 AHA/ACC guideline for the management of patients with valvular heart disease: a report of the American College of Cardiology/American Heart Association task force on practice guidelines. *J Am Coll Cardiol*. 2014;6 3:e57-185. https://doi.org/10.1016/j.jacc.2014.02.536
4. Nishimura RA, Otto CM, Bonow RO, Carabello BA, Erwin JP, Fleisher LA, et al. 2017 AHA/ACC focused update of the 2014 AHA/ACC guideline for the management of patients with valvular heart disease: a report of the American College of Cardiology/American Heart Association task force on clinical practice guidelines. *J Am Coll Cardiol*. 2017;70:252-89. https://doi.org/10.1016/j.jacc.2017.03.011
5. Acker MA, Parides MK, Perrault LP, Moskowitz AJ, Gelijns AC, Voisine P, et al. Mitral-valve repair versus replacement for severe ischemic mitral regurgitation. *N Engl J Med*. 2014;370:23-32. https://doi.org/10.1056/NEJMoa1312808
6. Goldstone AB, Cohen JE, Howard JL, Edwards BB, Acker AL, Hiesinger W, et al. A "repair-all" strategy for degenerative mitral valve disease safely minimizes unnecessary replacement. *Ann Thorac Surg*. 2015;99:1983-90; discussion: 1990. https://doi.org/10.1016/j.athoracsur.2014.12.076
7. Akins CW, Hilgenberg AD, Buckley MJ, Vlahakes GJ, Torchiana DF, Daggett WM, et al. Mitral valve reconstruction versus replacement for degenerative or ischemic mitral regurgitation. *Ann Thorac Surg*. 1994;58:668-75; discussion: 675. https://doi.org/10.1016/0003-4975(94)90725-0
8. Lee EM, Shapiro LM, Wells FC. Superiority of mitral valve repair in surgery for degenerative mitral regurgitation. *Eur Heart J*. 1997;18:655-63. https://doi.org/10.1093/oxfordjournals.eurheartj.a015312
9. David TE, Armstrong S, Ivanov J. Chordal replacement with polytetrafluoroethylene sutures for mitral valve repair: a 25-year experience. *J Thorac Cardiovasc Surg*. 2013;145:1563-9. https://doi.org/10.1016/j.jtcvs.2012.05.030
10. David TE, Omran A, Armstrong S, Sun Z, Ivanov J. Long-term results of mitral valve repair for myxomatous disease with and without chordal replacement with expanded polytetrafluoroethylene sutures. *J Thorac Cardiovasc Surg*. 1998;115: 1279-85; discussion: 1285. https://doi.org/10.1016/S0022-5223(98)70210-7
11. Pfannmueller B, Misfeld M, Verevkin A, Garbade J, Holzhey DM, Davierwala P, et al. Loop neochord versus leaflet resection techniques for minimally invasive mitral valve repair: long-term results. *Eur J Cardiothorac Surg*. 2021;59: 180-6. https://doi.org/10.1093/ejcts/ezaa255
12. Park MH, Zhu Y, Imbrie-Moore AM, Wang H, Marin-Cuartas M, Paulsen MJ, et al. Heart valve biomechanics: the frontiers of modeling modalities and the expansive capabilities of ex vivo heart simulation. *Front Cardiovasc Med*. 2021;8:673689. https://doi.org/10.3389/fcvm.2021.673689
13. Jensen MO, Siefert AW, Okafor I, Yoganathan AP. Measurement technologies for heart valve function. In: Sacks MS, Liao J, eds. *Advances in Heart Valve*

Biomechanics: Valvular Physiology, Mechanobiology, and Bioengineering. Springer International Publishing; 2018:115-49. https://doi.org/10.1007/978-3-030-01993-8_6

14. Ni XD, Huang J, Hu YP, Xu R, Yang WY, Zhou LM. Assessment of the rotation motion at the papillary muscle short-axis plane with normal subjects by two-dimensional speckle tracking imaging: a basic clinical study. *PLoS One*. 2013; 8:e83071. https://doi.org/10.1371/journal.pone.0083071
15. Imbrie-Moore AM, Park MH, Paulsen MJ, Sellke M, Kulkami R, Wang H, et al. Biomimetic six-axis robots replicate human cardiac papillary muscle motion: pioneering the next generation of biomechanical heart simulator technology. *J R Soc Interf*. 2020;17:20200614. https://doi.org/10.1098/rsif.2020.0614
16. Imbrie-Moore AM, Paulsen MJ, Thakore AD, Wang H, Hironaka CE, Lucian HJ, et al. Ex vivo biomechanical study of apical versus papillary neochord anchoring for mitral regurgitation. *Ann Thorac Surg*. 2019;108:90-7. https://doi.org/10.1016/j.athoracsur.2019.01.053
17. International Organization for Standardization. ISO 5840-1:2015 (En): Cardiovascular implants: cardiac valve prostheses. Accessed July 21, 2021. https://www.iso.org/obp/ui/#iso:std:iso:5840:-1:ed-1:v1:en
18. Wang H, Paulsen MJ, Imbrie-Moore AM, Tada Y, Bergamasco H, Baker SW, et al. In vivo validation of restored chordal biomechanics after mitral ring annuloplasty in a rare ovine case of natural chronic functional mitral regurgitation. *J Cardiovasc Dev Dis*. 2020;7:17. https://doi.org/10.3390/jcdd7020017
19. Paulsen MJ, Bae JH, Imbrie-Moore A, Wang H, Hironaka CE, Farry JM, et al. Development and ex vivo validation of novel force-sensing neochordae for measuring chordae tendineae tension in the mitral valve apparatus using optical fibers with embedded Bragg gratings. *J Biomech Eng*. 2020;142:0145011-9. https://doi.org/10.1115/1.4044142
20. Imbrie-Moore AM, Zhu Y, Park MH, Paulsen MJ, Wang H, Woo YJ. Artificial papillary muscle device for off-pump transapical mitral valve repair. *J Thorac Cardiovasc Surg*. November 30, 2020 [Epub ahead of print]. https://doi.org/10.1016/j.jtcvs.2020.11.105
21. Caballero A, Mao W, McKay R, Sun W. Transapical mitral valve repair with neochordae implantation: FSI analysis of neochordae number and complexity of leaflet prolapse. *Int J Numer Methods Biomed Eng*. 2020;36:e3297. https://doi.org/10.1002/cnm.3297
22. Jimenez JH, Soerensen DD, He Z, Ritchie J, Yoganathan AP. Mitral valve function and chordal force distribution using a flexible annulus model: an in vitro study. *Ann Biomed Eng*. 2005;33:557-66. https://doi.org/10.1007/s10439-005-1512-9
23. Gillinov AM, Cosgrove DM, Blackstone EH, Diaz R, Arnold JH, Lytle BW, et al. Durability of mitral valve repair for degenerative disease. *J Thorac Cardiovasc Surg*. 1998;116:734-43. https://doi.org/10.1016/S0022-5223(98)00450-4
24. Gunning GM, Murphy BP. Characterisation of the fatigue life, dynamic creep and modes of damage accumulation within mitral valve chordae tendineae. *Acta Biomater*. 2015;24:193-200. https://doi.org/10.1016/j.actbio.2015.06.015
25. Landsberg JW. Heart failure for the pulmonary critical care physician. In: *Clinical Practice Manual for Pulmonary and Critical Care Medicine*. Elsevier; 2018: 65-92. https://doi.org/10.1016/B978-0-323-39952-4.00006-8
26. Mielniczuk LM, Lamas GA, Flaker GC, Mitchell G, Smith SC, Gersh BJ, et al. Left ventricular end-diastolic pressure and risk of subsequent heart failure in patients following an acute myocardial infarction. *Congest Heart Fail*. 2007;13: 209-14. https://doi.org/10.1111/j.1527-5299.2007.06624.x
27. Dang MC, Thacker JG, Hwang JC, Rodeheaver GT, Melton SM, Edlich RF. Some biomechanical considerations of polytetrafluoroethylene sutures. *Arch Surg*. 1990;125:647-50. https://doi.org/10.1001/archsurg.1990.01410170095020
28. Catanese J, Cooke D, Maas C, Pruitt L. Mechanical properties of medical grade expanded polytetrafluoroethylene: the effects of internodal distance, density, and displacement rate. *J Biomed Mater Res*. 1999;48:187-92. https://doi.org/10.1002/(SICI)1097-4636(1999)48:2<187::AID-JBM13>3.0.CO;2-M
29. Sutton MG, Sharpe N. Left ventricular remodeling after myocardial infarction: pathophysiology and therapy. *Circulation*. 2000;101:2981-8. https://doi.org/10.1161/01.cir.101.25.2981
30. Burchfield JS, Xie M, Hill JA. Pathological ventricular remodeling: mechanisms: part 1 of 2. *Circulation*. 2013;128:388-400. https://doi.org/10.1161/CIRCULATIONAHA.113.001878

Key Words: mitral valve, neochordal repair, static pressurization assessment, diastolic phase inversion, cardiac biomechanics, robotic simulation

APPENDIX 1. SAMPLE SIZE ANALYSIS

To determine the appropriate sample size, a few initial exploratory tests were performed to evaluate the feasibility of the experimental setup as well as to analyze the magnitude of the obtained forces and the variance among them to determine the study sample size. Among these initial tests, we observed an expected mean paired difference of approximately 2 mm for neochordal length, an expected standard deviation of approximately 1 mm, an acceptance of the Shapiro–Wilk null hypothesis for normal distribution ($P > .05$), and a coefficient of variation >1. On the basis of the power analysis of the compared paired difference results of the exploratory tests, a total of $n = 5$ paired samples were enough to observe a significant difference at standard 95% confidence and 80% power levels. Therefore, we decided to perform a total of 6 paired ($n + 1$), independent tests for each neochord implantation condition to ensure adequate power.

TABLE E1. Hemodynamic, chordal force, and neochord length data

	Baseline	Prolapse	DPI repair	Physiologic repair
Pressure				
Transmitral mean back pressure, mm Hg	99.386	74.731	99.053	98.806
Mitral positive pressure time, s	0.432	0.465	0.411	0.446
Atrial RMS pressure, mm Hg	15.496	14.168	14.709	15.422
Atrial maximum pressure, mm Hg	46.886	40.709	44.614	45.740
Ventricular RMS pressure, mm Hg	65.586	57.465	65.385	66.109
Ventricular maximum pressure, mm Hg	121.352	113.108	123.286	123.460
Flow				
Heart rate, bpm	70	70	70	70
Pump stroke volume, mL	110.055	110.011	109.961	110.056
Systolic time, s	0.300	0.300	0.300	0.300
Systolic percent of cycle	34.961	35.007	34.974	34.961
Mitral forward flow time, s	0.524	0.518	0.520	0.527
Mitral cardiac output, L/min	5.408	4.225	5.337	5.524
Mitral forward volume, mL	85.051	88.983	87.798	88.760
Mitral closing volume, mL	−6.671	−10.233	−7.994	−7.757
Mitral leakage volume, mL	−1.119	−18.392	−3.567	−2.110
Mitral leakage rate, mL/s	−4.100	−68.790	−12.820	−7.764
Mitral mean flow, mL/s	161.431	171.006	167.645	167.391
Mitral RMS flow, mL/s	215.181	231.191	226.761	225.290
Mitral peak flow, mL/s	571.336	594.178	600.392	600.127
Mitral regurge fraction, %	9.014	31.158	13.335	11.087
Energy				
Ventricular energy (VE), mJ	990.308	927.776	998.139	992.598
Transmitral closing energy loss, mJ	17.698	44.786	30.275	29.586
Transmitral closing energy loss, % VE	1.795	4.904	3.013	2.973
Transmitral leakage energy loss, mJ	16.032	200.185	46.967	29.565
Transmitral leakage energy loss, % VE	1.630	21.873	4.714	2.974
Transmitral total energy loss, mJ	40.067	278.372	100.413	87.072
Transmitral total energy loss, % VE	3.972	30.521	9.928	8.652
Chordal data				
Neochord length, mm	N/A	N/A	16.42	14.22
Primary and secondary chordal forces, N	0.662	0.549	0.681	0.568

All information is presented as averaged across all 6 paired experiments. *DPI*, Diastolic phase inversion; *RMS*, root mean square; *bpm*, beats per minute; *VE*, ventricular energy.